

## COMMUNICATIONS

# An Efficient NMR Experiment for Analyzing Sugar-Puckering in Unlabeled DNA: Application to the 26-kDa Dead Ringer–DNA Complex

Junji Iwahara,<sup>1</sup> Jonathan M. Wojciak, and Robert T. Clubb<sup>1</sup>

*Department of Chemistry and Biochemistry, UCLA-DOE Laboratory of Structural Biology and Molecular Medicine, University of California, Los Angeles, 405 Hilgard Avenue, Los Angeles, California 90095-1570*

Received May 25, 2001; revised September 21, 2001; published online November 7, 2001

We present a new NMR experiment for estimating the type and degree of sugar-puckering in high-molecular-weight unlabeled DNA molecules. The experiment consists of a NOESY sequence preceded by a constant-time scalar coupling period. Two subexperiments are compared, each differing in the amount of time the  ${}^3J_{\text{H}3'/\text{H}2'}$  and  ${}^3J_{\text{H}3'/\text{H}2''}$  couplings are active on the H3' magnetization. The resultant data are easy to analyze, since a comparison of the signal intensities of any resolved NOE cross peak originating from H3' atoms of the duplex can be used to estimate the sum of the  ${}^3J_{\text{H}3'/\text{H}2'}$  and  ${}^3J_{\text{H}3'/\text{H}2''}$  couplings and thus the puckering type of the deoxyribose ring. Isotope filters to eliminate signals of the  ${}^{13}\text{C}$ -labeled component in the F1-dimension are implemented, facilitating analyses of high-molecular-weight protein–DNA complexes containing  ${}^{13}\text{C}$ -labeled protein and unlabeled DNA. The utility of the experiment is demonstrated on the 26-kDa Dead Ringer protein–DNA complex and reveals that the DNA uniformly adopts the S-type configuration when bound to protein. © 2001 Elsevier Science

**Key Words:** DNA; isotope filter; *J* modulation; protein–DNA complex; NMR; sugar pucker.

Deoxyribose rings in DNA adopt two principal conformations: S- and N-type sugar-puckers (1). Since the energy barrier between these conformers is small (~4 kcal/mol) (2), they rapidly interconvert in solution. Hydrated molecular dynamics simulations of B-form DNA suggest that repuckering occurs approximately every 0.1 ns, with the transition requiring only a few picoseconds (3, 4). While in the absence of protein the dominant conformer in B-form DNA is the S-type (typically greater than 75% of the species at equilibrium) (e.g., 5), the furanose ring has been shown to alter its structure to adaptively recognize proteins (6–9). Several NMR methods for analyzing sugar-puckering in small unlabeled DNA molecules in the absence of protein are available (10, 11). However, they are largely ineffective for the study of higher molecular weight systems in either the free-state

or bound to protein. Recently new methods have been employed to study sugar-puckering in high-molecular-weight systems, but these methods require  ${}^{13}\text{C}$ -labeling of the DNA (6, 12–14). Since the vast majority of NMR studies of protein–DNA complexes are performed on samples consisting of carbon-13- and nitrogen-15-labeled protein and unlabeled DNA, we have developed a simple and efficient NMR experiment for measuring sugar-puckering in protein–DNA complexes that does not require  ${}^{13}\text{C}$ -labeled DNA.

To estimate the type and degree of sugar-puckering of unlabeled DNA molecules in protein DNA complexes, we constructed the pulse sequences shown in Fig. 1. Each sequence is essentially a two-dimensional (2D) F1- ${}^{13}\text{C}$  filtered NOESY experiment that incorporates a constant-time period in which the coupling between the H2'/H2'' and the H1' and H3' atoms of the deoxyribose ring are active for differing amounts of time. A comparison of the signal intensities of the appropriate NOE cross peaks therefore provides an estimate of the scalar couplings between these atoms and provides a quick and simple method of estimating the type and degree of puckering. We call this new experiment JUNSY, for *J*-utilization in NOE spectroscopy.

The JUNSY consists of two subexperiments, which differ in the relative positioning of rectangular and selective shaped proton 180° pulses. In the following argument, we discuss the behavior of NOE cross peaks originating from only the H3' protons of the DNA molecule, since these cross peaks are of primary importance in estimating the values of  ${}^3J_{\text{H}3'/\text{H}2'}$  and  ${}^3J_{\text{H}3'/\text{H}2''}$ . It is important to note that data from these two experiments display only intra-DNA and intermolecular protein–DNA NOEs, since intramolecular protein NOE cross peaks are eliminated by a F1- ${}^{13}\text{C}$ -filtering scheme (15). In each subexperiment the scalar couplings described by  ${}^3J_{\text{H}3'/\text{H}2'}$ ,  ${}^3J_{\text{H}3'/\text{H}2''}$ , and  ${}^3J_{\text{H}3'/\text{H}4'}$  are active on the transverse magnetization of the H3' atoms between points a and b. The REBURP 180° pulse (16) is selective for the H1', H3', and H4' resonances located between 4.0 and 6.2 ppm and does not significantly perturb the signals originating from the

<sup>1</sup> To whom correspondence should be addressed. E-mail: iwahara@mbi.ucla.edu or rclubb@mbi.ucla.edu.

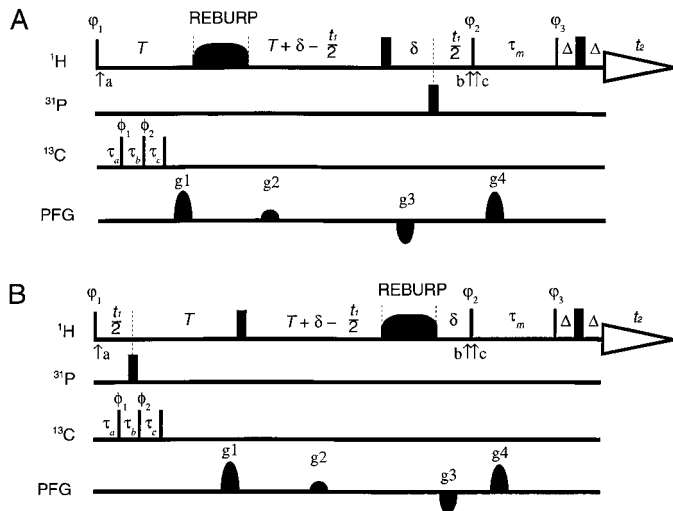


**FIG. 1.** Pulse sequences of the JUNS Y experiment. Two experiments A and B should be run in an interleaved manner. Narrow and bold lines indicate high-power  $90^\circ$  and  $180^\circ$  pulses, respectively ( $^1\text{H}$ , 33.8 kHz at 5.0 ppm;  $^{13}\text{C}$ , 19 kHz at 70 ppm;  $^{31}\text{P}$ , 19 kHz at 0 ppm). Unless indicated, the pulse phase is  $x$ . The  $^1\text{H}$  carrier position set at 5.0 ppm is close to the center of the  $\text{H1}'$ ,  $\text{H3}'$ ,  $\text{H4}'$  region. The REBURP  $180^\circ$  pulse is selective for  $\text{H1}'$ ,  $\text{H3}'$ , and  $\text{H4}'$  resonances and does not affect resonances from the  $\text{H2}'$  and  $\text{H2}''$  atoms. On a 500-MHz spectrometer the pulse length and the maximum  $\gamma B_1/2\pi$  of this pulse were 4.0 ms and 1.6 kHz, respectively. The phase of the REBURP pulse was adjusted to achieve the same phase as the rectangular  $180^\circ$  pulses.  $^{13}\text{C}$  pulses are applied to eliminate signals from  $^{13}\text{C}$ -bound protons in the F1 dimension, which is useful in analysis of DNA bound to a  $^{13}\text{C}$ -labeled protein. Delays of  $\tau_a$ ,  $\tau_b$ , and  $\tau_c$  for the F1- $^{13}\text{C}$ -filter scheme are 3.0, 3.5, and 4.0 ms, respectively. Phase cycling was as follows:  $\phi_1 = \{4x, 4(-x)\}$ ,  $\phi_2 = \{8x, 8(-x)\}$ ,  $\phi_3 = \{x, y, -x, -y\}$ .  $\phi_1 = \{x, -x\}$ ,  $\phi_2 = \{2x, 2(-x)\}$ , receiver =  $\{x, -y, -x, y, 2(-x, y, x, -y), x, -y, -x, y\}$ . The quadrature detection in the  $t_1$  domain was achieved by alternating  $\phi_1$  and receiver phases in the States-TPPI manner. The spin-echo period immediately before acquisition  $\{\Delta - ^1\text{H}180^\circ - \Delta\}$  is optional and was included to obtain better baselines. If omitted, the receiver phase should be  $\{-x, -y, x, y, 2(x, y, -x, -y), -x, -y, x, y\}$ . Gradient conditions were as follows:  $g_1$  (0.5 ms; 20.0 G/cm),  $g_2$  (0.5 ms; 8.6 G/cm),  $g_3$  (0.5 ms;  $-11.4$  G/cm),  $g_4$  (1.0 ms; 25.7 G/cm). The gradient powers of  $g_1$ ,  $g_2$ , and  $g_3$  must satisfy the condition of  $g_2 = g_1 + g_3$ . The delays of  $T$ ,  $\delta$ ,  $\tau_m$ , and  $\Delta$  are 22 ms, 1.5 ms, 200 ms, and 100  $\mu\text{s}$ , respectively. Weak presaturation was applied on the HDO resonance during the repetition delay and the  $^1\text{H}$  carrier position was jumped to 5.0 ppm just before the first  $^1\text{H}$   $90^\circ$  pulse. To minimize contributions to the NOE cross-peak intensities other than the desired scalar coupling effects, it is important that the rectangular and REBURP  $180^\circ$  pulses be of correct duration and relative phase. Application of the pulsed field gradients  $g_1$ ,  $g_2$ ,  $g_3$  compensates for imperfection in these  $180^\circ$  pulses. These gradients dephase the transverse magnetizations that are not refocused by  $^1\text{H}$   $180^\circ$  pulses, while the  $g_3$  gradient rephases the desired magnetization. Therefore, cross peaks in the JUNS Y experiment are observed only within the selective bandwidth of the  $^1\text{H}$  REBURP pulse in the F1 dimension. The  $^{31}\text{P}$  pulses eliminate  $^1\text{H}$ - $^{31}\text{P}$  scalar couplings providing better sensitivity. However, the  $^{31}\text{P}$  pulses are not essential and their presence or absence does not affect the  $I_B/I_A$  ratio.

$\text{H2}'$  and  $\text{H2}''$  atoms, which typically resonate between 1.8 and 2.9 ppm. The judicious placement of the REBURP pulse therefore enables the selective manipulation of the  $^3J_{\text{H3}'\text{H2}'}$  and  $^3J_{\text{H3}'\text{H2}''}$  couplings between points a and b of the sequence. The intensity of NOE cross peaks originating from the  $\text{H3}'$  atoms in the F1 dimension of each experiment is modulated by scalar

coupling and transverse relaxation of the in-phase transverse  $\text{H3}'$  magnetization. The attenuation of these signals can be described by a factor  $q$ ,

$$q_A = \cos(2\pi^3 J_{\text{H3}'\text{H2}'}\delta)\cos(2\pi^3 J_{\text{H3}'\text{H2}''}\delta) \\ \times \cos\{\pi^3 J_{\text{H3}'\text{H4}'}(2T + 2\delta)\} \exp\{-R_2(2T + 2\delta) \\ - R^* \tau_{\text{REBURP}}\}, \quad [1]$$

$$q_B = \cos(2\pi^3 J_{\text{H3}'\text{H2}'}T)\cos(2\pi^3 J_{\text{H3}'\text{H2}''}T) \\ \times \cos\{\pi^3 J_{\text{H3}'\text{H4}'}(2T + 2\delta)\} \exp\{-R_2(2T + 2\delta) \\ - R^* \tau_{\text{REBURP}}\}, \quad [2]$$

where  $q_A$  and  $q_B$  represent the attenuation of the  $\text{H3}'$  signal in the A and B subexperiments, respectively;  $R_2$  is the transverse relaxation rate of the  $\text{H3}'$  atom; and  $R^*$  is the rate of relaxation during the REBURP pulse applied for duration  $\tau_{\text{REBURP}}$  ( $\sim 4.0$  ms). We ignore the effects of strong coupling in this analysis, since scalar couplings involving the  $\text{H1}'$  or  $\text{H3}'$  protons are expected to satisfy the weak coupling condition, regardless of the pucker type. Inspection of Eqs. [1]–[2] reveals that in the two subexperiments the amount of transverse  $\text{H3}'$  magnetization at point b is identical, except for differing cosine dependencies on the  $^3J_{\text{H3}'\text{H2}'}$  and  $^3J_{\text{H3}'\text{H2}''}$  couplings (in subexperiments A and B, the couplings are active for times  $2\delta$  and  $2T$ , respectively). The remainder of each subexperiment is composed of a NOE mixing period in which the transverse proton magnetization present at point b is used to generate off-diagonal NOESY cross peaks by dipolar relaxation with proximal protons. Since in each subexperiment the NOESY transfer periods are identical, their spectra are identical except that the NOE cross peaks originating from the  $\text{H3}'$  atoms in the F1 dimension are attenuated differently. A measure of the extent of this disparate attenuation can be obtained by comparing the signal intensities of NOE cross peaks between any hydrogen atom frequency labeled in the F2 dimension and the  $\text{H3}'$  atom frequency labeled in the F1 dimension. The cross-peak intensity ratio is described by

$$I_B/I_A = q_B/q_A = \cos(2\pi^3 J_{\text{H3}'\text{H2}'}T)\cos(2\pi^3 J_{\text{H3}'\text{H2}''}T)/ \\ \{\cos(2\pi^3 J_{\text{H3}'\text{H2}'}\delta)\cos(2\pi^3 J_{\text{H3}'\text{H2}''}\delta)\}, \quad [3]$$

where  $I_A$  and  $I_B$  are the intensities of NOE cross peaks ( $\text{F1}$ ,  $\text{H3}'$  atom;  $\text{F2}$ , any proton atom) in subexperiments A and B, respectively. It is important to note that the ratio is independent of the distance between the two nuclei and the effects of spin diffusion, enabling the use of relatively large  $\tau_m$  values for increased sensitivity.

An estimation of the sugar-pucker type can be obtained by analysis of the  $I_B/I_A$  ratio. Because deoxyribose rings rapidly interconvert between the N- and S-type conformers, the observed sugar proton scalar coupling constants are an ensemble average

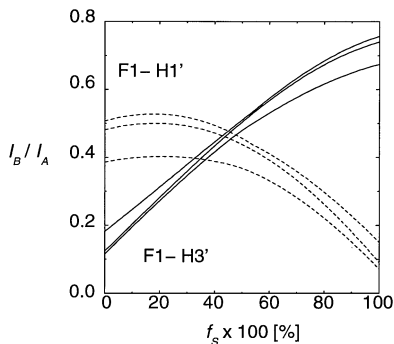


**FIG. 2.** The relation between the peak intensity ratio  $I_B/I_A$  and the fraction of S-type sugar-pucker ( $f_S$ ) in the interconversion equilibrium between N- and S-type puckers. Solid and dashed lines represent the intensity ratios of cross peaks frequency labeled in the F1 dimension with chemical shifts of the H3' and H1' resonances, respectively. The ranges of the pseudorotation phase angles  $p$  for N- and S-type puckers are  $0^\circ \leq p_N \leq 36^\circ$  and  $144^\circ \leq p_S \leq 180^\circ$ , respectively. The amplitude of the pucker is assumed to be  $36^\circ$ . For each nucleus, the upper and lower lines represent the maximum and minimum expected  $I_B/I_A$  values for the extreme ranges of  $p_N$  and  $p_S$ . The center lines were calculated assuming  $p_N = 9^\circ$  and  $p_S = 162^\circ$ , the energy-minima for N- and S-type puckers, respectively (2). The theoretical values for the coupling constants were obtained from Altona and co-workers (5). The fraction of N-type pucker is  $100 \times (1 - f_S) \%$ . Experimental conditions shown in Fig. 1 are assumed.

given by

$$J_{obs} = f_S J_S + f_N J_N, \quad [4]$$

where  $J_S$  and  $J_N$  are the scalar coupling constants of pure S- and N-type puckers and  $f_S$  and  $f_N$  are the fractions of these puckers in the ensemble (5, 11). The expected values of  $I_B/I_A$  as a function of  $f_S$  are plotted in Fig. 2 and have been derived using Eqs. [3]–[4] and the theoretical values of the  $^3J_{H3'H2'}$  and  $^3J_{H3'H2''}$  couplings in S- and N-type DNA (5). Inspection reveals that the  $I_B/I_A$  ratios of NOE cross peaks involving the H3' atom (frequency labeled in the F1 dimension) are  $\sim 0.2$  for N-type puckers that have pseudorotation angles ranging between  $0^\circ$  and  $36^\circ$ , and  $\sim 0.7$  for S-type puckers that have pseudorotation angles between  $144^\circ$  and  $180^\circ$ . An analysis of cross peak intensities of NOEs involving the H1' proton (frequency labeled in the F1 dimension) is also useful. Using the same line of reasoning employed to derive Eqs. [1]–[3], the intensities ratios of H1' NOE cross peaks can be shown to depend on the scalar coupling constants  $^3J_{H1'H2'}$  and  $^3J_{H1'H2''}$ . Figure 2 shows a plot of the expected values of the  $I_B/I_A$  ratio of NOE cross peaks involving the H1' atoms (frequency labeled in the F1 dimension) as a function of  $f_S$ . Cross peaks to the H1' atoms have an opposite and smaller dependence on the pucker type, and therefore provide a convenient check of the puckering information derived from analysis of the H3' NOE cross peaks.

Analysis of the intensity ratios of cross peaks involving the H3' protons provides a rapid method for estimating the range of pseudorotation angles that the deoxyribose ring adopts. It is

important to note that this approach is much easier and more efficient than analyzing homonuclear COSY-type data. First, the JUNSY experiment provides a greater chance to obtain information about the sugar-pucker compared to homonuclear COSY-type experiments. In COSY-type data only a limited number of through-bond correlations are observed. In contrast, any resolved NOE cross peak involving the H3' atom frequency labeled in the F1 dimension can be used to analyze puckering in the JUNSY experiment. In practice, both intra- and internucleotide NOE cross peaks between the H3' protons frequency labeled in the F1 dimension and the H1', H2'/H2'', CH<sub>3</sub>, H6, or H8 protons labeled in the F2 dimension can be used. The NOESY based JUNSY experiment is also significantly more sensitive than COSY-type experiments. This is because cross peaks in COSY data have an antiphase multiplet fine structure, which suffers from peak cancellation effects as the line width increases (11); in contrast the JUNSY experiment has cross peaks with in-phase lineshapes.

To demonstrate the utility of the JUNSY experiment, we recorded each subexperiment on a 26-kDa ARID<sup>F355L</sup>-DNA complex. The complex consists of <sup>13</sup>C-, <sup>15</sup>N-labeled AT-rich interaction domain from the Dead Ringer protein (residues Gly262 to Gly398, with a phenylalanine to leucine mutation at position 355 (ARID<sup>F355L</sup>)) and an unlabeled 15-bp DNA fragment dissolved in 100% D<sub>2</sub>O (17). NMR measurements were performed at 37°C on a Bruker DRX-500 spectrometer using an  $\sim 1.4$  mM sample of the complex. The spectral widths in the F1 and F2 dimensions were 10.0 and 13.0 ppm, respectively. A total of 216\* and 1024\* complex points were acquired in the  $t_1$  and  $t_2$  domains, respectively. The two subexperiments A and B (Fig. 1) were recorded in an interleaved manner with 128 scans per FID, resulting in a total measurement time of  $\sim 46$  h. The NMR data were processed and analyzed using NMRPipe (18) and NMRView (19), respectively.

The JUNSY spectrum of the ARID<sup>F355L</sup>-DNA complex is shown in Fig. 3. Three regions of the spectrum are plotted, demonstrating that for each H3' resonance, several cross peaks can be used to estimate the type of puckering. For example, guanine-30 exhibits resolved cross peaks from its H3' atom to its own H8 atom (Fig. 3A), to its own H1' atom (Fig. 3B), and to its own H2' and H2'' atoms (Fig. 3C). Since these cross peaks are resolved, they provide a reliable measure of  $f_S$ . The high sensitivity of the JUNSY experiment may appear to be surprising at first, given the fact that the H3' magnetization in both experiments is transverse between points a and b for a total of 47 ms ( $2T + 2\delta$ , where  $T$  and  $\delta$  are 22 and 1.5 ms, respectively). However, a low density of protons encircles the H3' atoms in B-form DNA, resulting in slow transverse relaxation rates (in the ARID<sup>F355L</sup>-DNA complex the H3' atoms on average have  $T_2$  relaxation time constants of  $\sim 42$  ms (data not shown)). Since proton transverse relaxation rates are roughly proportional to the rotational correlation time of a macromolecule, we anticipate that our experiment will be useful for protein-DNA complexes up to  $\sim 35$  kDa.

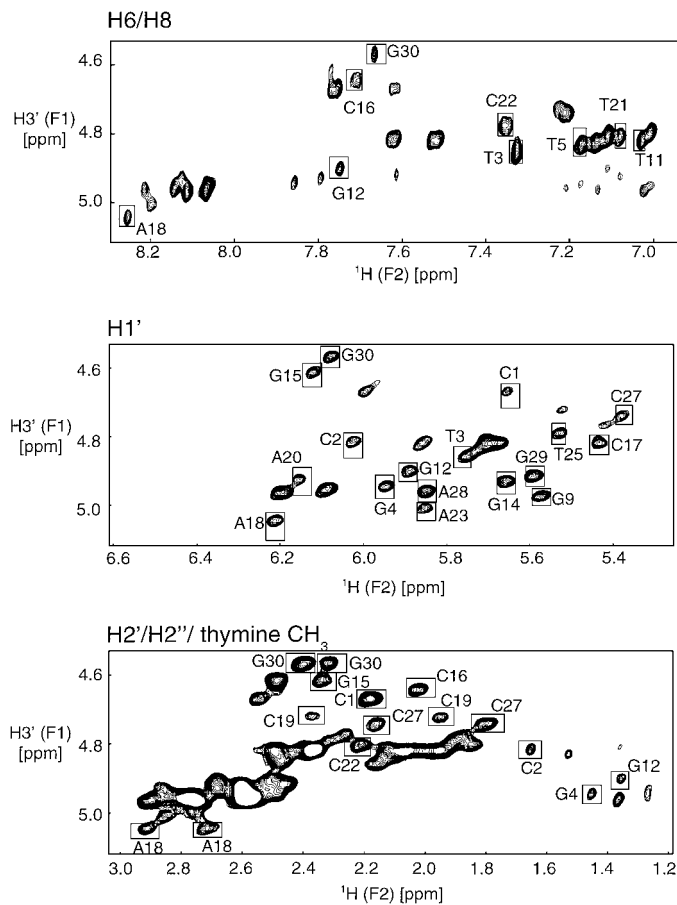


**FIG. 3.** Representative NMR spectra of the JUNSY experiment. The figure shows data from subspectrum A (Fig. 1A) recorded on the 26-kDa ARID<sup>F355L</sup>-DNA complex dissolved in D<sub>2</sub>O. Three regions of the spectrum are plotted showing F1-frequency labeled cross peaks of the H3' atoms to H6/H8 atoms (Fig. 3A); to H1' atoms (Fig. 3B); and to H2', H2'', and CH<sub>3</sub> atoms (Fig. 3C). Isolated NOE cross peaks involving H3' resonances frequency labeled in the F1 dimension are enclosed in boxes and are used in the generation of Table 1.

Table 1 lists the measured values of  $f_S$  for the ARID<sup>F355L</sup>-DNA complex. There are a total of 30 nucleotides in the duplex, 29 of which exhibited resolved cross peaks enabling their  $f_S$  values to be estimated. The data clearly reveal that the S-type pucker is the dominant form in the complex. The majority of nucleotides exhibit  $f_S$  values greater than 70%, while the remaining 6 have  $f_S$  values between 56 and 68%. Of the latter, 4 are located at the ends of the DNA and are presumably more mobile in solution, enabling facile switching between the N- and S-type conformers. Nucleotides C22 and C27 are located toward the center of the duplex and also exhibit  $f_S$  values smaller than 70%. They may be slightly perturbed by the presence of the bound ARID<sup>F355L</sup> protein, but more likely may represent the higher intrinsic preference of deoxycytidine to adopt the N-type conformer that has been predicted by *ab initio* calculations (2, 20). It is important to note that we confirmed the results of the JUNSY experiment by carefully analyzing the pattern of intra-

and internucleotide proton distances derived from NOE build-up curves of the complex (17, 21) (data not shown). Although the ARID<sup>F355L</sup>-DNA complex does not contain any N-type sugar-puckers in it, the JUNSY experiment should readily identify these pucker types as well. This is because the experiment relies on distinct frequency differences between the H1'/H3'/H4' atoms and the H2'/H2'' atoms, which are preserved in both S- and N-type configurations (14). However, it is likely that the JUNSY experiment will exhibit lower sensitivity for DNA adopting N-type puckers. This is because, the  $^3J_{H3'H4'}$  coupling attenuates the relevant signal (Eqs. [1]–[2]), and this coupling is significantly larger in N-type puckers (S-type  $^3J_{H3'H4'} = 0.8$  Hz, N-type  $^3J_{H3'H4'} = 8.6$  Hz (5)). This problem can be overcome

**TABLE 1**  
Intensity Ratios  $I_B/I_A$  and Calculated  $f_S$  of the Dead Ringer ARID<sup>F355L</sup>-DNA Complex

| DNA residue     | $I_B/I_A^a$    |                | 100 × $f_S$ [%]      |                      |         |
|-----------------|----------------|----------------|----------------------|----------------------|---------|
|                 | H3'(F1)        | H1'(F1)        | H3'(F1) <sup>b</sup> | H1'(F1) <sup>c</sup> | Average |
| <b>Strand 1</b> |                |                |                      |                      |         |
| C1              | 0.56 ± 0.02    | 0.43 ± 0.06    | 59 ± 4               | 52 ± 20              | 56      |
| C2              | 0.70 ± 0.05    | 0.33 ± 0.05    | 87 ± 13              | 71 ± 9               | 79      |
| T3              | 0.69 ± 0.05    | 0.31 ± 0.04    | 84 ± 11              | 73 ± 6               | 79      |
| G4              | 0.68 ± 0.08    | 0.21 ± 0.04    | 82 ± 17              | 87 ± 5               | 85      |
| T5              | 0.64 ± 0.07    | — <sup>d</sup> | 73 ± 17              | —                    | 73      |
| A6              | — <sup>d</sup> | 0.30 ± 0.09    | —                    | 75 ± 15              | 75      |
| T7              | — <sup>d</sup> | 0.32 ± 0.08    | —                    | 72 ± 14              | 72      |
| T8              | — <sup>d</sup> | — <sup>d</sup> | —                    | —                    | —       |
| G9              | 0.87 ± 0.06    | 0.31 ± 0.05    | 100 <sup>e</sup>     | 73 ± 7               | 86      |
| A10             | 0.76 ± 0.03    | — <sup>d</sup> | 100 ± 5              | —                    | 100     |
| T11             | 0.69 ± 0.05    | 0.30 ± 0.05    | 85 ± 11              | 75 ± 8               | 80      |
| G12             | 0.73 ± 0.07    | 0.32 ± 0.06    | 96 ± 19              | 72 ± 12              | 84      |
| T13             | — <sup>d</sup> | 0.33 ± 0.06    | —                    | 71 ± 11              | 71      |
| G14             | 0.77 ± 0.06    | 0.28 ± 0.03    | 100 ± 10             | 78 ± 5               | 89      |
| G15             | 0.55 ± 0.04    | — <sup>d</sup> | 57 ± 7               | —                    | 57      |
| <b>Strand 2</b> |                |                |                      |                      |         |
| C16             | 0.55 ± 0.05    | 0.41 ± 0.03    | 58 ± 9               | 56 ± 8               | 58      |
| C17             | 0.80 ± 0.05    | 0.32 ± 0.05    | 100 <sup>e</sup>     | 72 ± 8               | 86      |
| A18             | 0.81 ± 0.07    | 0.22 ± 0.05    | 100 ± 6              | 85 ± 6               | 89      |
| C19             | 0.68 ± 0.09    | 0.31 ± 0.05    | 82 ± 18              | 73 ± 7               | 79      |
| A20             | 0.74 ± 0.10    | 0.27 ± 0.08    | 100 ± 27             | 79 ± 12              | 90      |
| T21             | — <sup>d</sup> | 0.30 ± 0.07    | —                    | 75 ± 11              | 75      |
| C22             | 0.61 ± 0.05    | — <sup>d</sup> | 68 ± 10              | —                    | 68      |
| A23             | 0.79 ± 0.08    | 0.30 ± 0.05    | 100 ± 10             | 75 ± 8               | 86      |
| A24             | 0.70 ± 0.04    | 0.28 ± 0.05    | 87 ± 13              | 78 ± 7               | 83      |
| T25             | 0.67 ± 0.08    | — <sup>d</sup> | 80 ± 20              | —                    | 80      |
| A26             | — <sup>d</sup> | 0.24 ± 0.04    | —                    | 83 ± 4               | 83      |
| C27             | 0.57 ± 0.06    | 0.33 ± 0.03    | 61 ± 6               | 70 ± 8               | 66      |
| A28             | 0.81 ± 0.06    | — <sup>d</sup> | 100 <sup>e</sup>     | —                    | 100     |
| G29             | 0.73 ± 0.06    | 0.28 ± 0.04    | 96 ± 27              | 78 ± 7               | 87      |
| G30             | 0.60 ± 0.06    | — <sup>d</sup> | 65 ± 12              | —                    | 65      |

<sup>a</sup> The peak heights were used for calculating the ratios. Error estimation was based on the standard deviation of the noise in the spectra.

<sup>b,c</sup> The values of  $f_S$  are calculated with  $I_B/I_A$  using conditions of the center lines in Fig. 2. The precision is also shown, which was estimated with  $I_B/I_A$  error.

<sup>d</sup>  $I_B/I_A$  could not be measured due to peak overlap or errors greater than 0.1.

<sup>e</sup> Error values cannot be determined, but the ratio value indicates  $f_S$  of ~100%.

by shortening the delay  $T$  at the expense of the number of  $t_1$  data points that can be recorded.

In conclusion, we have developed a new experiment for investigating deoxyribose ring puckering in large unlabeled DNA molecules and demonstrated its utility on a 26-kD protein–DNA complex. The experiment is designed to assess ring puckering in protein–DNA complexes consisting of  $^{13}\text{C}$ -,  $^{15}\text{N}$ -labeled proteins and unlabeled DNA, the most commonly used samples in NMR studies of protein–DNA complexes. The resultant data provide important information about the puckering state of the deoxyribose ring, enabling more accurate and precisely determined solution structures to be obtained (22). It should be noted that while this paper was being reviewed a related constant-time NOESY experiment that measures vicinal  $\text{H}3'$ - $\text{P}$  couplings was published (23), suggesting that the constant-time NOESY approach will be of general use for the measurement of other scalar and dipolar couplings.

#### ACKNOWLEDGMENTS

We thank Dr. Robert Peterson for technical support and Dr. Juli Feigon for useful discussions. This work was supported by a grant from the U.S. Department of Energy (DE-FC-03-87ER60615).

#### REFERENCES

1. W. Saenger, "Principles of Nucleic Acid Structure," Springer-Verlag, New York (1984).
2. N. Foloppe and A. D. MacKerell, Intrinsic conformational properties of deoxyribonucleosides: Implicated role for cytosine in the equilibrium among the A, B, and Z forms of DNA, *Biophys. J.* **76**, 3206–3218 (1999).
3. T. E. Cheatham, III and P. A. Kollman, Molecular dynamics simulation of nucleic acids, *Annu. Rev. Phys. Chem.* **51**, 435–471 (2000).
4. B. Hartmann and R. Lavery, DNA structural forms, *Quart. Rev. Biophys.* **29**, 309–368 (1996).
5. J. van Wijk, B. D. Huckriede, J. H. Ippel, and C. Altona, Furanose sugar conformations in DNA from NMR coupling constants, *Methods Enzymol.* **211**, 286–306 (1992).
6. T. Szyperski, C. Fernández, A. Ono, M. Kainosho, and K. Wüthrich, Measurement of deoxyribose  $^3J_{\text{HH}}$  scalar couplings reveals protein binding-induced changes in the sugar-puckers of the DNA, *J. Am. Chem. Soc.* **120**, 821–822 (1998).
7. Y.-G. Gao, S.-Y. Su, H. Robinson, S. Padmanabhan, L. Lim, B. S. McCrary, S. P. Edmondson, J. W. Shriver, and A. H.-J. Wang, The crystal structure of the hyperthermophile chromosomal protein Sso7d bound to DNA, *Nature Struct. Biol.* **5**, 782–786 (1998).
8. J. L. Kim and S. K. Burley, 1.9 Å resolution refined structure of TBP recognizing the minor groove of TATAAAG, *Nature Struct. Biol.* **1**, 638–653 (1994).
9. H. Robinson, Y.-G. Gao, B. S. McCrary, S. P. Edmondson, J. W. Shriver, and A. H.-J. Wang, The hyperthermophile chromosomal protein Sac7d sharply kinks DNA, *Nature* **392**, 202–205 (1998).
10. L. J. Rinkel and C. Altona, Conformational analysis of the deoxyribofuranose ring in DNA by means of sums of proton-proton coupling constants: A graphical method, *J. Biomol. Struct. Dyn.* **4**, 621–649 (1987).
11. H. Widmer and K. Wüthrich, Simulated two-dimensional NMR cross-peak fine structures for  $^1\text{H}$  spin systems in polypeptides and polydeoxynucleotides, *J. Magn. Reson.* **74**, 316–336 (1987).
12. J. Boisbouvier, B. Brutscher, A. Pardi, D. Marion, and J.-P. Simorre, NMR determination of sugar-puckers in nucleic acids form CSA—dipolar cross-correlated relaxation, *J. Am. Chem. Soc.* **122**, 6779–6780 (2000).
13. I. C. Feli, C. Richter, C. Griesinger, and H. Schwalbe, Determination of RNA sugar pucker mode from cross-correlated relaxation in solution NMR spectroscopy, *J. Am. Chem. Soc.* **121**, 1956–1957 (1999).
14. A. P. Dejaegere and D. A. Case, Density functional study of ribose and deoxyribose chemical shifts, *J. Phys. Chem. A* **102**, 5280–5289 (1998).
15. G. M. Clore, E. C. Murphy, A. M. Gronenborn, and A. Bax, Determination of three-bond  $^1\text{H}3'$ - $^{31}\text{P}$  couplings in nucleic acids and protein-nucleic acid complexes by quantitative J correlation spectroscopy, *J. Magn. Reson.* **134**, 164–167 (1998).
16. H. Geen and R. Freeman, Band-selective radiofrequency pulses, *J. Magn. Reson.* **93**, 93–141 (1991).
17. J. Iwahara, J. M. Wojciak, and R. T. Clubb, Improved NMR spectra of a protein–DNA complex through rational mutagenesis and the application of a sensitivity optimized isotope-filtered NOESY experiment, *J. Biomol. NMR* **19**, 231–241 (2001).
18. F. Delaglio, S. Grzesiek, G. W. Vuister, G. Zhu, J. Pfeifer, and A. Bax, NMRPipe—A multidimensional spectral processing system based on UNIX pipes, *J. Biomol. NMR* **6**, 277–293 (1995).
19. B. A. Johnson and R. A. Blevins, NMR View—A computer program for the visualization of NMR data, *J. Biomol. NMR* **4**, 603–614 (1994).
20. T. E. Cheatham, III, P. Cieplak, and P. A. Kollman, A modified version of the Cornell et al. force field with improved sugar-pucker phase and helical repeat, *J. Biomol. Struct. Dyn.* **16**, 845–862 (1999).
21. S. S. Wijmenga, M. M. W. Mooren, and C. W. Hilbers, NMR of nucleic acids: From spectrum to structure, in "NMR of Macromolecules: A Practical Approach" (G. C. K. Roberts, Ed.), pp. 216–288, IRL Press, Oxford (1993).
22. C. Fernández, T. Szyperski, M. Billeter, A. Ono, H. Iwai, M. Kainosho, and K. Wüthrich, Conformational changes of the BS2 operator DNA upon complex formation with the *Antennapedia* homeodomain studied by NMR with  $^{13}\text{C}/^{15}\text{N}$ -labeled DNA, *J. Mol. Biol.* **292**, 609–617 (1999).
23. Z. Wu, N. Tjandra, and A. Bax, Measurement of  $^1\text{H}3'$ - $^{31}\text{P}$  dipolar couplings in a DNA oligonucleotide by constant-time NOESY difference spectroscopy, *J. Biomol. NMR* **19**, 367–370 (2001).